

# An $N$ -Body Solver for Square Root Iteration

Matt Challacombe,<sup>\*</sup> Terry Haut,<sup>†</sup> and Nicolas Bock<sup>‡</sup>

*Theoretical Division, Los Alamos National Laboratory*

We develop the Sparse Approximate Matrix Multiply  $n$ -body solver for first order Newton Schulz iteration of the matrix square root and inverse square root. The solver performs an  $n$ -body occlusion-cull, yeilding a bounded relative error in the matrix-matrix product and reduced complexity for problems with structured metric decay. This complexity reduction cooresponds to the hierarchical resolution of algebraic structures within recursive volume of the product, a consequence of metric locality. For square root iteration, strongly localized sub-volumes are culled about plane-diagonals and along the cube-diagonal, cooresponding to resolution of the identity.

The main contributions of this paper are bounds on the SpAMM product and demonstration of a new algebraic locality that develops in these sub-volumes with strongly contractive identity iteration. This contraction cooresponds to the deflation of sub-volumes onto plane diagonals of the resolvent, and to a stronger bound on the SpAMM product.

Also, we carry out a first order Fréchet analyses for single and dual channel instances of the square root iteration, and look at bifurcations due to ill-conditioning and a too-agresive SpAMM approximation. Then, we show that extreme SpAMM approximations and strongly contractive identity iteration can be achieved through iterated regularization, and demonstrate the potential for orders of magnitude acceleration with product representation of the inverse factor.

## I. INTRODUCTION

In many areas of application, long range, high value correlations lead to matrix equations with decay properties. By decay, we mean an approximate inverse relationship between matrix elements and an associated distance; this may be a simple inverse relationship between matrix elements and the Cartesian distance between corresponding support functions, or it may involve a non-Euclidean distance, *e.g.* a generalized measure between character strings in a training library [].

Matrix equations with decay have history and recent development in the statistics and statistical physics literature [1–5]. Also recently, methods for meshfree interpolation are demonstrating remarkable predictive power through delocalized correlations and cooresponding ill-conditioned matrix equations with extreme slow decay [], a problem equivalent to the LCAO Gaussian basis problem in quantum chemistry []. Generally, local support functions are correlated through Lowdin’s symmetric orthogonalization based on the matrix inverse square root [6, 7], yeilding representation independent matrix equations. In electronic structure, important long-range correlations manifest in slow decay properties of the gap shifted matrix sign function, as projector of the effective Hamiltonian (Fig. I). Both of these matrix problem with decay, the matrix sign function and the matrix inverse

square root, are related by Higham’s identity:

$$\text{sign} \left( \begin{bmatrix} 0 & s \\ I & 0 \end{bmatrix} \right) = \begin{bmatrix} 0 & s^{1/2} \\ s^{-1/2} & 0 \end{bmatrix}. \quad (1)$$

The theory and computation of these matrix functions is given in Higham’s reference [8].

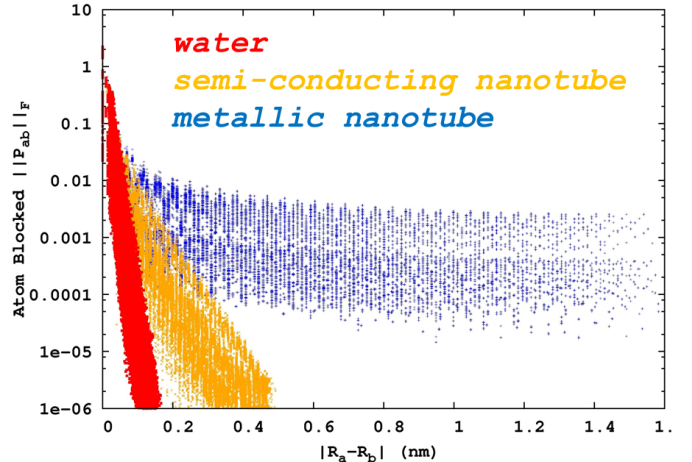


FIG. 1: Examples from electronic structure of decay for the spectral projector (gap shifted sign function) with respect to local (atomic) support. Shown is decay for systems with correlations that are short (insulating water), medium (semi-conducting 4,3 nanotube), and long (metallic 3,3 nanotube) ranged, from exponential (insulating) to algebraic (metallic).

<sup>\*</sup>Electronic address: matt.challacombe@freeon.org; URL: <http://www.freeon.org>

<sup>†</sup>Electronic address: haut@lanl.gov

<sup>‡</sup>Electronic address: nicolasbock@freeon.org; URL: <http://www.freeon.org>

A well conditioned matrix  $s$  may often correspond to matrix sign and inverse square root functions with rapid exponential decay, and be amenable to *ad hoc* matrix truncation or “sparsification”,  $\bar{s} = s + \epsilon_\tau^s$ , where  $\epsilon_\tau^s$  is the error introduced according to some criterion  $\tau$ . The criterion  $\tau$  might be a drop-tolerance,  $\epsilon_\tau^s = \{-s_{ij} * \hat{e}_i | |s_{ij}| <$

$\tau\}$ , a radial cutoff,  $\epsilon_\tau^s = \{-s_{ij} * \hat{e}_i \mid \|r_i - r_j\| > \tau\}$ , or some other approach to truncation, perhaps involving a sparsity pattern chosen *a priori* for computational expedience. Then, the sparse general matrix-matrix multiply (SpGEMM) [9–12] may be employed, yielding fast solutions for multiplication rich iterations with fill-in modulated by truncation. Comprehensive surveys of these methods in the numerical linear algebra are given by Benzi [13, 14], and by Bowler [15] and Benzi [16] for electronic structure.

Often however, matrix truncation is ineffective for ill-conditioned problems, because of slow decay, and because of increased numerical sensitivities to poorly controled (absolute) truncation errors, *e.g.* in the matrix-product:

$$\overline{\mathbf{a} \cdot \mathbf{b}} = \mathbf{a} \cdot \mathbf{b} + \epsilon_\tau^a \cdot \mathbf{b} + \mathbf{a} \cdot \epsilon_\tau^b + \mathcal{O}(\tau^2). \quad (2)$$

An alterative approach is to find a reduced rank approximation closed under the opperations of interest [? ]. However, compression to a reduced rank may be expensive if the rank is not much much smaller than the dimension. Both of these methods, truncation and rank reduction, are focused on matrix data as the target for compresion. In this contribution, our target for compression is instead the matrix product itself. For problems with decay, we show that an underlying metric locality, together with a new form of algebraic locality, can lead to complexity reduction under contractive iteration and the  $n$ -body occlusion-cull. The organization of this paper follows.

## Contents

<b>I. Introduction</b>	1
<b>II. Sparse Approximate Matrix Multiplication (SpAMM)</b>	2
A. Occlusion-Cull	2
B. Bound	3
C. Related Research	3
<b>III. First Order Newton-Shulz Iteration</b>	4
A. Sign Iteration	4
B. Square Root Iteration	4
C. Logistic Map	5
D. Instance and Stability	5
<b>IV. Error Flows in Square Root Iteration</b>	6
A. Cannonical, Dual Channel Instance	6
B. Single Channel Instance	6
C. Bifurcations	6
<b>V. TEMPERRY:NOTES FOR REGULARIZATION SECTION</b>	6

<b>VI. Iterated Regularization</b>	8
<b>VII. Locality</b>	9
<b>VIII. Summary</b>	10
<b>IX. Conclusions</b>	11
<b>A. Implementation</b>	12
<b>B. Data</b>	12
<b>References</b>	12

## II. SPARSE APPROXIMATE MATRIX MULTIPLICATION (SpAMM)

In this contribution, we consider an  $N$ -body approach to the approximation of matrix functions with decay, based on the quadtree data structure [? ? ]

$$\mathbf{a}^i = \begin{bmatrix} \mathbf{a}_{00}^{i+1} & \mathbf{a}_{01}^{i+1} \\ \mathbf{a}_{10}^{i+1} & \mathbf{a}_{11}^{i+1} \end{bmatrix}, \quad (3)$$

and orderings that are locality preserving []. Orderings that preserve data locality are well developed and *generic* in the database theory [], providing fast spatial and metric queries. Locality enabled, fast data access is central to  $b$ -body approximations [], and an important problem for enterprise [] and runtime systems [], moreso with memory hierarchies becoming increasingly asynchronous and decentralized [? ]. For matrices with decay, orderings that preserve locality lead to blocked-by-magnitude matrix structures with well segregated neighborhoods, inhabited by matrix elements of like size, and efficiently resolved by the quadtree data structure [].

### A. Occlusion-Cull

The Sparse Approximate Matrix Multiply (SpAMM) carries out occlusion-culling to find only the most important sub-volumes in an approximate matrix product. SpAMM has evolved from a row-coloumn oriented skipout mechanism within the BCSR and DBCSR structures [], to hierarchical approaches based on the quadtree and related to the occlusion-culling found in advanced mechanics and graphics methodologies [], with occlusion the avoidance of unessesary tree-work and culling the collection of significant tasks. Here, we ammend the SpAMM occlusion-cull with the recursion:

$$\mathbf{a}^i \otimes_{\tau} \mathbf{b}^i = \begin{cases} \emptyset & \text{if } \|\mathbf{a}^i\| \|\mathbf{b}^i\| < \tau \|\mathbf{a}\| \|\mathbf{b}\| \\ \mathbf{a}^i \cdot \mathbf{b}^i & \text{if } (\mathbf{i} = \text{leaf}) \\ \left[ \mathbf{a}_{00}^{i+1} \otimes_{\tau} \mathbf{b}_{00}^{i+1} + \mathbf{a}_{01}^{i+1} \otimes_{\tau} \mathbf{b}_{10}^{i+1}, \quad \mathbf{a}_{00}^{i+1} \otimes_{\tau} \mathbf{b}_{01}^{i+1} + \mathbf{a}_{01}^{i+1} \otimes_{\tau} \mathbf{b}_{11}^{i+1} \right] & \text{else} \\ \left[ \mathbf{a}_{00}^{i+1} \otimes_{\tau} \mathbf{b}_{01}^{i+1} + \mathbf{a}_{01}^{i+1} \otimes_{\tau} \mathbf{b}_{11}^{i+1}, \quad \mathbf{a}_{00}^{i+1} \otimes_{\tau} \mathbf{b}_{01}^{i+1} + \mathbf{a}_{01}^{i+1} \otimes_{\tau} \mathbf{b}_{11}^{i+1} \right] & \text{else} \end{cases}, \quad (4)$$

which bounds the relative occlusion error

$$\frac{\|\Delta_{\tau}^{a \cdot b}\|}{n^2} \leq \tau \|\mathbf{a}\| \|\mathbf{b}\|, \quad (5)$$

that occurs in the approximate product

$$\widetilde{\mathbf{a} \cdot \mathbf{b}} \equiv \mathbf{a} \otimes_{\tau} \mathbf{b} = \mathbf{a} \cdot \mathbf{b} + \Delta_{\tau}^{a \cdot b}, \quad (6)$$

where  $\|\cdot\| \equiv \|\cdot\|_F$  is a sub-multiplicative norm  $\|\cdot\|$ .

## B. Bound

We now prove (5).

**Proposition 1.** Let  $\tau_{A,B} = \tau \|\mathbf{A}\| \|\mathbf{B}\|$ . Then for each  $i,j$ ,

$$\left| (A \otimes_{\tau} B)_{ij} - (A \cdot B)_{ij} \right| \leq n \tau_{A,B},$$

and

$$\|A \otimes_{\tau} B - A \cdot B\|_F \leq n^2 \tau_{A,B}.$$

*Proof.* We first show the following technical result: it is possible to choose  $\alpha_{lij} \in \{0, 1\}$  such that

$$(A \otimes_{\tau} B)_{ij} = \sum_{l=1}^n A_{il} B_{lj} \alpha_{lij}, \quad (7)$$

In addition, if  $\alpha_{lij} = 0$ , then  $|A_{il}| |B_{lj}| < \tau_{A,B}$ . To show this, we use induction on the number  $k_{\max}$  of levels.

First, if  $k_{\max} = 0$ ,

$$A \otimes_{\tau} B = \begin{cases} 0 & \text{if } \|\mathbf{A}\|_F \|\mathbf{B}\|_F < \tau_{A,B}, \\ A \cdot B & \text{else.} \end{cases}$$

Therefore,  $A \otimes_{\tau} B$  is of the form (7) with either all  $\alpha_{lij} = 0$  or all  $\alpha_{lij} = 1$ . Moreover, if  $\alpha_{lij} = 0$ , then  $|A_{il}| |B_{lj}| \leq \|\mathbf{A}\|_F \|\mathbf{B}\|_F < \tau_{A,B}$ .

Now assume that the claim holds for  $k_{\max} - 1$ . We show that it holds for  $k_{\max}$ . Indeed, if  $\|\mathbf{A}\|_F \|\mathbf{B}\|_F < \tau_{A,B}$ , we have that  $A \otimes_{\tau} B = 0$ , which is of the form (7) with all  $\alpha_{lij} = 0$ . Also, if  $\alpha_{lij} = 0$ , then  $|A_{il}| |B_{lj}| < \|\mathbf{A}\|_F \|\mathbf{B}\|_F < \tau_{A,B}$ .

Now assume that  $\|\mathbf{A}\|_F \|\mathbf{B}\|_F \geq \tau_{A,B}$ . Then

$$A \otimes_{\tau} B = \begin{pmatrix} A_{11} \otimes_{\tau} B_{11} + A_{12} \otimes_{\tau} B_{21} & A_{11} \otimes_{\tau} B_{12} + A_{12} \otimes_{\tau} B_{22} \\ A_{21} \otimes_{\tau} B_{11} + A_{22} \otimes_{\tau} B_{21} & A_{21} \otimes_{\tau} B_{12} + A_{22} \otimes_{\tau} B_{22} \end{pmatrix}.$$

We need to consider four cases:  $i \leq n/2$  and  $j \leq n/2$ ,  $i > n/2$  and  $j > n/2$ ,  $i > n/2$  and  $j \leq n/2$ , and, finally,  $i > n/2$  and  $j > n/2$ . Since the analysis is similar for all four cases, we only consider  $i \leq n/2$  and  $j \leq n/2$ . We have that

$$\begin{aligned} (A \otimes_{\tau} B)_{ij} &= (A_{11} \otimes_{\tau} B_{11} + A_{12} \otimes_{\tau} B_{21})_{ij} \\ &= \sum_{l=1}^{n/2} (A_{11})_{il} (B_{11})_{lj} \alpha_{lij}^{(1)} + \\ &\quad \sum_{l=1}^{n/2} (A_{12})_{il} (B_{21})_{lj} \alpha_{lij}^{(2)} \\ &= \sum_{l=1}^n A_{il} B_{lj} \alpha_{lij}, \end{aligned}$$

where we used the induction hypothesis in the second equality.

Now suppose that  $\alpha_{lij} = 0$  for some  $l$ . Then  $\tilde{\alpha}_{lij}^{(1)} = 0$  if  $l \leq n/2$  or  $\tilde{\alpha}_{l-n/2,ij}^{(2)} = 0$  if  $l > n/2$ . If, e.g.,  $\tilde{\alpha}_{l-n/2,ij}^{(2)} = 0$ , then  $|A_{il}| |B_{lj}| = |(A_{12})_{i,l-n/2}| |(B_{21})_{l-n/2,j}| < \tau_{A,B}$ , where we used the induction hypothesis in the final inequality. The analysis for  $l \leq n/2$  is similar, and the claim follows.

We can now finish the proof of Proposition 1. Indeed, by (7),

$$\begin{aligned} \left| (A \otimes_{\tau} B)_{ij} - (A \cdot B)_{ij} \right| &\leq \sum_{l=1}^n |A_{il} B_{lj}| |\alpha_{lij} - 1| \\ &= \sum_{\alpha_{lij}=0} |A_{il} B_{lj}|. \end{aligned}$$

In addition, if  $\alpha_{lij} = 0$ , then  $|A_{il} B_{lj}| < \tau_{A,B}$  and the lemma follows.  $\square$

## C. Related Research

SpAMM is perhaps most closely related to the Strassen-like branch of fast matrix multiplication [17, 18]. In

the Strassen-like approach, disjoint volumes in (abstract) tensor intermediates are omitted recursively [1]. In the SpAMM approach to fast multixplication, the numerically most significant volumes in naïve  $(ijk)$  tensor intermediates are culled, with error bounded by Eq. (5). This bound makes  $\otimes_\tau$  a *single* form of fast multiplication, as explained by Demmel, Dumitriu and Holz (DDH; Ref. [?]).

SpAMM is a  $n$ -body method for fast matrix multiplication, related to the generalized methods popularized by Grey [19, 20]. In our development, generalization reflects the *genericity* [1] of recursive data access [1], enabling range queries, metric queries, higher dimensional queries and so on, with common frameworks, structures and runtimes. So far, we have prototyped  $n$ -body solvers for the five mainstay solvers in modern electronic structure theory, involving Fock exchange [1], semi-local exchange-correlation functionals [1], the Hartree (Coulomb) interaction [1], matrix sign function [1] and the matrix inverse square root (this work). This contribution is cornerstone for the simplification and evolution of these solvers.

Also,  $n$ -body methods offer well established protocols for turning spatial and metric locality into data and temporal locality [1]; recently, x, y and Yellik showed perfect strong scaling and communication optimality for pairwise  $n$ -body methods [? ]. Bridging the gap between  $n$ -body solver and fast matrix multiplication, we recently demonstrated strong scaling for fast matrix multiplication (SpAMM) [1]. In this work, we demonstrate additional **algebraic locality** principles that may further enhance locality of reference and high performance implementations.

Noted by Aluru [1], top-down  $n$ -body recursion and breadth-first map-reduction may be viewed as two sides of the same database problem [1]. Alignment with emergent enterprise frameworks and database trends [1] and functional programming languages that support genericity [1] may enable decentralized commodity concurrence [1] as well as software sustainability [? ].

This work offers a data local alternative to fast non-deterministic methods for sampling the product, which include sketching [21–26], joining [27–33], sensing [1] and probing [1]. These methods involve a weighted (probabilistic) and on the fly sampling, with the potential for complexity reduction in the case of random distributions. SpAMM also employs on the fly weighted sampling, but with compression through locality, brought about by algebraic correlations (towards identity) and also in the metric structure, through strong Euclidean locality.

Methods that achieve compression in the stream of product intermediates are different from reduced rank algorithms that achieve matrix compression in a step that precedes multiplication (separability) [1]. However, matrix compressions are generally compatible with the quadtree, as are additional fast (generalized) solvers that add complex functionality (*e.g.* in electronic structure theory [1]). Thus, generality and interoperability may enable deeply layered, thin and generic solvers easy access

to in place data. Further, language support may provide simple (skeletonized) frameworks for generic recursion, offering opportunities to greatly simplify codebase at the systems level, lowering barriers to entry and enhancing concurrence (in the Erlang sense).

Finally, previous work on the scaled NS iteration has heavily influenced this work. Formost is Higham, Mackey, Mackey and T (HMMT; Ref. [1]) masterwork on convergence of NS iteration under all groups, wherein HMMT also develop Fréchet analyses for single square root iteration at the fixed point. Also, important inspiration comes from Chen and Chow’s [1] approach to scaled NS iteration for ill-conditioned problems [1], and from the Helgaker groups work on NS iteration, whose notation we follow in part [1].

### III. FIRST ORDER NEWTON-SHULZ ITERATION

There are two common, first order NS iterations; the sign iteration and the square root iteration, related by the square,  $\mathbf{I}(\cdot) = \text{sign}^2(\cdot)$ . These equivalent iterations converge linearly at first, then enter a basin of stability marked by super-linear convergence. Our interest is to access this basin with the most permissive  $\tau$  possible, building a foundation for future refinement at a reduced cost and with a higher precision ( $\tau \rightarrow 0$ ) [? ].

#### A. Sign Iteration

For the NS sign iteration, this basin is marked by a behavioral change in the difference  $\delta\mathbf{X}_k = \widetilde{\mathbf{X}}_k - \mathbf{X}_k = \text{sign}(\mathbf{X}_{k-1} + \delta\mathbf{X}_{k-1}) - \text{sign}(\mathbf{X}_{k-1})$ , where  $\delta\mathbf{X}_{k-1}$  is some previous error. The change in behavior is associated with the onset of idempotence and the bounded eigenvalues of  $\text{sign}'(\cdot)$ , leading to single iteration when  $\text{sign}'(\mathbf{X}_{k-1}) \delta\mathbf{X}_{k-1} < 1$ . Global perturbative bounds on this iteration have been derived by Bai and Demmel [34], while Byers, He and Mehrmann [1] developed asymptotic bounds. The automatic stability of sign iteration is a well developed theme in Ref.[8].

#### B. Square Root Iteration

In this work, we are concerned with resolution of the identity [1]

$$\mathbf{I}(\mathbf{s}) = \mathbf{s}^{1/2} \cdot \mathbf{s}^{-1/2}, \quad (8)$$

and the corresponding canonical (dual) square root iteration [1];

$$\begin{aligned} \mathbf{y}_k &\leftarrow h_\alpha [\mathbf{y}_{k-1} \cdot \mathbf{z}_{k-1}] \cdot \mathbf{y}_{k-1} \\ \mathbf{z}_k &\leftarrow \mathbf{z}_{k-1} \cdot h_\alpha [\mathbf{y}_{k-1} \cdot \mathbf{z}_{k-1}], \end{aligned} \quad (9)$$

with eigenvalues in the proper domain aggregated towards 0 or 1 by the NS map  $h_\alpha[\mathbf{x}] = \frac{\sqrt{\alpha}}{2}(3 - \alpha\mathbf{x})$  [1]. Then, starting with  $\mathbf{z}_0 = \mathbf{I}$  and

$$\mathbf{s} \leftarrow \mathbf{s}/s_{N-1},$$

$$\mathbf{x}_0 = \mathbf{y}_0 = \mathbf{s}, \mathbf{y}_k \rightarrow s^{1/2}, \mathbf{z}_k \rightarrow s^{-1/2} \text{ and } \mathbf{x}_k \rightarrow \mathbf{I}.$$

As in the case of sign iteration, this dual iteration was shown by Higham, Mackey, Mackey and Tisseur [35] to remain bounded in the superlinear regime, by idempotent Frechet derivatives about the fixed point  $(\mathbf{s}^{1/2}, \mathbf{s}^{-1/2})$ , in the direction  $(\delta\mathbf{y}_{k-1}, \delta\mathbf{z}_{k-1})$ :

$$\delta\mathbf{y}_k = \frac{1}{2}\delta\mathbf{y}_{k-1} - \frac{1}{2}\mathbf{s}^{1/2} \cdot \delta\mathbf{z}_{k-1} \cdot \mathbf{s}^{1/2} \quad (10)$$

$$\delta\mathbf{z}_k = \frac{1}{2}\delta\mathbf{z}_{k-1} - \frac{1}{2}\mathbf{s}^{-1/2} \cdot \delta\mathbf{y}_{k-1} \cdot \mathbf{s}^{-1/2}. \quad (11)$$

In this contribution, we consider another aspect of convergence, namely the (hopefully) linear approach towards stability of the iteration

$$\tilde{\mathbf{x}}_k \leftarrow \tilde{\mathbf{y}}_k(\tilde{\mathbf{x}}_{k-1}) \otimes_\tau \tilde{\mathbf{z}}_k(\tilde{\mathbf{x}}_{k-1}), \quad (12)$$

made difficult by ill-conditioning and a sketchy  $\otimes_\tau$ .

### C. Logistic Map

Initially,  $h'_\alpha$  at the smallest eigenvalue  $x_0$  controls the rate of progress towards idempotence. As recently shown by Jie and Chen [36], for very ill-conditioned problems, a factor of two reduction in the number of NS steps can be achieved by choosing  $\alpha \sim 2.85$ , which is at the edge of stability. As argued by Pan and Schreiber [37], Jie and Chen [36], switching or damping the scaling factor towards  $\alpha = 1$  at convergence is important, shifting emphasis away from the behavior of  $x_0$  towards e.g.  $x_i \in [0.01, 1]$ , emphasizing overall convergence of the broad distribution [?]. In an approximate algebra like SpAMM, the potential for eigenvalues to fluctuate out of the domain of convergence must be considered. This is addressed in Section ??.

### D. Instance and Stability

There are a number of nominally equivalent instances of the square root iteration, related by commutations and transpositions. However, these instances may have very different stability properties, controlled to first order by the Frechet derivatives

$$\mathbf{x}_{\delta\hat{\mathbf{y}}_{k-1}} = \lim_{\tau \rightarrow 0} \frac{\mathbf{x}(\mathbf{y}_{k-1} + \tau\delta\hat{\mathbf{y}}_{k-1}, \mathbf{z}_{k-1}) - \mathbf{x}_k}{\tau} \quad (13)$$

and

$$\mathbf{x}_{\delta\hat{\mathbf{z}}_{k-1}} = \lim_{\tau \rightarrow 0} \frac{\mathbf{x}(\mathbf{y}_{k-1}, \mathbf{z}_{k-1} + \tau\delta\hat{\mathbf{z}}_{k-1}) - \mathbf{x}_k}{\tau}, \quad (14)$$

along the unit directions of the previous errors  $\delta\hat{\mathbf{y}}_{k-1}$  and  $\delta\hat{\mathbf{z}}_{k-1}$ , corresponding to the associated displacement

magnitudes  $\delta y_{k-1} = \|\delta\mathbf{y}_{k-1}\|$  and  $\delta z_{k-1} = \|\delta\mathbf{z}_{k-1}\|$ . Then, the differential

$$\delta\mathbf{x}_k = \mathbf{x}_{\delta\hat{\mathbf{y}}_{k-1}} \times \delta y_{k-1} + \mathbf{x}_{\delta\hat{\mathbf{z}}_{k-1}} \times \delta z_{k-1} + \mathcal{O}(\tau^2) \quad (15)$$

determines the total first order stability.

This formulation allows to consider orientational effects involving eigenvector fidelity and convergence of derivatives towards zero separately from displacement effects involving accumulation and SpAMM source errors. In some cases, instabilities may be associated with derivatives that do not vanish towards identity, yielding an unbounded iteration [1]. In other instances, an instability may be associated with rapidly increasing displacements, due to a too large  $\tau$ . Instability may also arise due to the numerical corruption of the eigenvectors, also resulting in derivatives that vanish too slowly (or blow up altogether).

The potential for instability is increased with ill-conditioning through the terms  $\|\mathbf{z}_k\| \rightarrow \sqrt{\kappa(\mathbf{s})}$ . Also for ill-conditioned systems, scaling is necessary to accelerate convergence. However with scaling, increasing the map derivative  $h'_\alpha$  can also further enhance the rate of error accumulation.

In following sections, we'll examine how these effects differ from the ideal (double precision) canonical (dual) square root iteration for ill-conditioned systems and in the strongly non-associative, sketchy  $\otimes_\tau$  regime corresponding to permissive values of  $\tau$ . At this early stage, we are interested in hazards and opportunities associated with different formulations and implementational details. In addition to deviations from the full precision dual instance, we will develop the “single” instance,

$$\begin{aligned} \mathbf{z}_k &\leftarrow \mathbf{z}_{k-1} \cdot h_\alpha[\mathbf{x}_{k-1}], \\ \mathbf{x}_k &\leftarrow \mathbf{z}_k^\dagger \cdot \mathbf{s} \cdot \mathbf{z}_{k-1}, \end{aligned} \quad (16)$$

with the corresponding differential;

$$\delta\mathbf{x}_k = \mathbf{x}_{\delta\hat{\mathbf{z}}_{k-1}} \times \delta z_{k-1} + \mathcal{O}(\tau^2). \quad (17)$$

Nominally,  $\mathbf{y}^{\text{dual}}$  is equivalent to  $\mathbf{y}_k^{\text{single}} \equiv \mathbf{z}_k^\dagger \cdot \mathbf{s}$  is also equivalent to  $\mathbf{y}_k^{\text{naive}} \equiv \mathbf{z}_k \cdot \mathbf{s}$ . However, with ill-conditioning and in only double precision, these two instances may diverge due to non-associative errors that rapidly compound. In the case of the duals iteration under SpAMM approximation, the  $\tilde{\mathbf{y}}_k^{\text{dual}}$  channel does not retain contact with the eigenvectors, span  $\mathbf{s}$ , whilst the single instance does. In the duals iteration, the  $\tilde{\mathbf{y}}_k$  SpAMM update is mild, with errors in the relative product remaining well conditioned. In the single instance, connection with  $\mathbf{s}$  is retained at each step, but at the price of the  $\mathbf{y}_k^{\text{single}}$  update involving magnitudes that vary widely in the SpAMM product.

## IV. ERROR FLOWS IN SQUARE ROOT ITERATION

### A. Canonical, Dual Channel Instance

Referring back to Eq. (15), we develop the Fréchet analyses [] with the goal of understanding the contractive approach to identity in competition with error accumulations and SpAMM sources. Of interest are the derivatives

$$\begin{aligned} \mathbf{x}_{\delta\hat{\mathbf{y}}_{k-1}} &= h_\alpha[\mathbf{x}_{k-1}] \cdot \delta\hat{\mathbf{y}}_{k-1} \cdot \mathbf{z}_k \\ &\quad + h'_\alpha \delta\hat{\mathbf{y}}_{k-1} \cdot \mathbf{z}_{k-1} \cdot \mathbf{y}_{k-1} \cdot \mathbf{z}_k \\ &\quad + \mathbf{y}_k \cdot \mathbf{z}_{k-1} \cdot h'_\alpha \delta\hat{\mathbf{y}}_{k-1} \cdot \mathbf{z}_{k-1}. \end{aligned} \quad (18)$$

$$\begin{aligned} \mathbf{x}_{\delta\hat{\mathbf{z}}_{k-1}} &= \mathbf{y}_{k-1} \cdot h'_\alpha \delta\hat{\mathbf{z}}_{k-1} \cdot \mathbf{y}_{k-1} \cdot \mathbf{z}_k \\ &\quad + \mathbf{y}_k \cdot \delta\hat{\mathbf{z}}_{k-1} \cdot h_\alpha[\mathbf{x}_{k-1}] \\ &\quad + \mathbf{y}_k \cdot \mathbf{z}_{k-1} \cdot \mathbf{y}_{k-1} \cdot h'_\alpha \delta\hat{\mathbf{z}}_{k-1}. \end{aligned} \quad (19)$$

Closer to a fixed point orbit,  $\mathbf{y}_k \cdot \mathbf{z}_{k-1} \rightarrow \mathbf{I}$ ,  $\mathbf{y}_{k-1} \cdot \mathbf{z}_k \rightarrow \mathbf{I}$ ,  $h_\alpha[\mathbf{x}_k] \rightarrow \mathbf{I}$  and  $h'_\alpha \rightarrow -\frac{1}{2}$  [?]. Then,

$$\mathbf{x}_{\delta\hat{\mathbf{y}}_{k-1}} \rightarrow \delta\hat{\mathbf{y}}_{k-1} \cdot (\mathbf{z}_k - \mathbf{z}_{k-1}) \quad (20)$$

and

$$\mathbf{x}_{\delta\hat{\mathbf{z}}_{k-1}} \rightarrow (\mathbf{y}_k - \mathbf{y}_{k-1}) \cdot \delta\hat{\mathbf{z}}_{k-1}. \quad (21)$$

Thus, contributions along  $\delta\hat{\mathbf{y}}_{k-1}$  and  $\delta\hat{\mathbf{z}}_{k-1}$  are tightly shut down in the region of superlinear convergence. Achieving a contractive fixed point orbit, however requires that the three terms in Eq. (??), with potentially different error accumulations and SpAMM sources, must cancel faster than  $\delta y_{k-1}$  and  $\delta z_{k-1}$  accumulate.

In this analysis, we've separated the directional component of the error from its distance, because in addition to the previous compounding error, each displacement contains also a first order SpAMM source error. Its simpler to consider these effects separately, at least in this first contribution.

To understand  $\delta z_{k-1}$ , we partially unwind the approximate  $\tilde{\mathbf{z}}_{k-1}$ ;

$$\tilde{\mathbf{z}}_{k-1} = \tilde{\mathbf{z}}_{k-2} \otimes_\tau h_\alpha[\tilde{\mathbf{x}}_{k-2}] \quad (22)$$

$$= \Delta_{\tilde{\mathbf{z}}_{k-2} \cdot h_\alpha[\tilde{\mathbf{x}}_{k-2}]} + \tilde{\mathbf{z}}_{k-2} \cdot h_\alpha[\tilde{\mathbf{x}}_{k-2}] \quad (23)$$

Then, using

$$h_\alpha[\tilde{\mathbf{x}}_{k-2}] = h_\alpha[\mathbf{x}_{k-2}] + h'_\alpha \delta \mathbf{x}_{k-2} \quad (24)$$

and taking  $\mathbf{z}_{k-1}$  from both sides, we find

$$\begin{aligned} \delta z_{k-1} &= \Delta_{\tilde{\mathbf{z}}_{k-2} \cdot h_\alpha[\tilde{\mathbf{x}}_{k-2}]} \\ &\quad + \delta \mathbf{z}_{k-2} \cdot h_\alpha[\tilde{\mathbf{x}}_{k-2}] + \mathbf{z}_{k-2} \cdot h'_\alpha \delta \mathbf{x}_{k-2}, \end{aligned} \quad (25)$$

bounded by

$$\begin{aligned} \delta z_{k-1} &< \|z_{k-2}\| (\tau \|h_\alpha[\tilde{\mathbf{x}}_{k-2}]\| + h'_\alpha \delta y_{k-2} \|z_{k-2}\|) \\ &\quad + \delta z_{k-2} (\|h_\alpha[\tilde{\mathbf{x}}_{k-2}]\| + \|y_{k-2}\|). \end{aligned} \quad (26)$$

primary error channels contributing to  $\delta z_{k-1}$  are through the first order SpAMM error  $\tau \|z_{k-2}\| \|h_\alpha[\tilde{\mathbf{x}}_{k-2}]\|$  and the volatile term  $h'_\alpha \delta y_{k-2} \|z_{k-2}\|^2$ .

corresponding to basis corruption and controlled by  $\otimes_{\tau_s}$ , with  $\tau_s \ll \tau$ . As above, we can unwind this sensitive term, to find

$$\begin{aligned} \delta y_{k-2} &< \|y_{k-3}\| (\tau_s \|h_\alpha[\tilde{\mathbf{x}}_{k-3}]\| + h'_\alpha \delta z_{k-3}) \\ &\quad + \delta y_{k-3} (\|\tilde{\mathbf{z}}_{k-3}\| + \|h_\alpha[\tilde{\mathbf{x}}_{k-3}]\|). \end{aligned} \quad (27)$$

### B. Single Channel Instance

Here, we carry on from Eq. (17) in the “single” instance, with the single channel differential

$$\mathbf{x}_{\hat{\mathbf{z}}_{k-1}} = \hat{\mathbf{z}}_{k-1}^\dagger \cdot \mathbf{s} \cdot \mathbf{z}_k + \mathbf{z}_k^\dagger \cdot \mathbf{s} \cdot \mathbf{z}_{\hat{\mathbf{z}}_{k-1}} \quad (28)$$

$$\begin{aligned} \mathbf{z}_{\hat{\mathbf{z}}_{k-1}} &= \delta \hat{\mathbf{z}}_{k-1} \cdot h_\alpha[\tilde{\mathbf{x}}_{k-1}] + \mathbf{z}_{k-1} \cdot ( \\ &\quad h'_\alpha \delta \hat{\mathbf{z}}_{k-1}^\dagger \cdot \mathbf{s} \cdot \mathbf{z}_{k-1} + \mathbf{z}_{k-1}^\dagger \cdot \mathbf{s} \cdot h'_\alpha \delta \hat{\mathbf{z}}_{k-1}) \end{aligned} \quad (29)$$

$$\tilde{\mathbf{y}}_{k-1}^{\text{single}} = \tilde{\mathbf{z}}_{k-1}^\dagger \otimes_\tau \mathbf{s} \quad (30)$$

$$= \Delta \tilde{\mathbf{z}}_{k-1}^\dagger \cdot \mathbf{s} + (\tilde{\mathbf{z}}_{k-2} \cdot h_\alpha[\tilde{\mathbf{x}}_{k-2}])^\dagger \cdot \mathbf{s} \quad (31)$$

### C. Bifurcations

Differences in occlusion between single and dual magnified as bounds for s.z not as tight as bounds for h.y.

\*lot\* of overlap too (reproducing hilberts etc).

## V. TEMPORARY:NOTES FOR REGULARIZATION SECTION

The idea of preconditioning is that we can use a low tolerance  $\tau_0$  (e.g.  $\tau_0 = 10^{-2}$ ) to cheaply obtain an approximation  $R_0 \approx S^{-1/2}$ . Then since  $S_1 \equiv R_0 S R_0$  is close to the identity matrix  $I$ ,

$$\|R_0 S R_0 - I\|_F \lesssim \tau_0,$$

we can use Newton Schulz on  $S_1$  with a higher tolerance  $\tau_1$  to get an accurate approximation  $R_1 = S_1^{-1/2}$  and using only a few iterations:

$$\|R_1 S_1 R_1 - I\|_F \lesssim \tau_1.$$

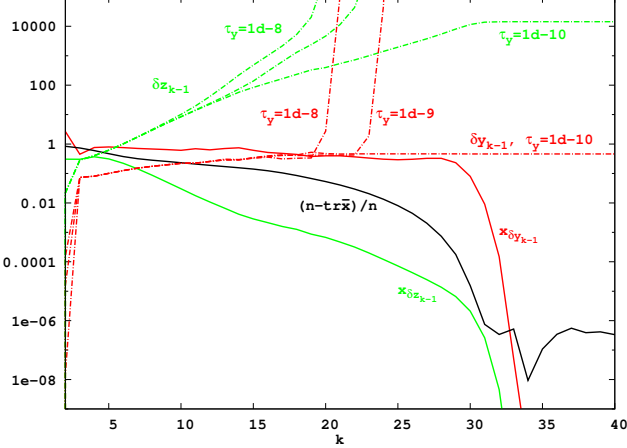


FIG. 2: Derivatives, displacements and the approximate trace of the unscaled, dual NS iteration for a (3,3) nanotube with  $\kappa = 10^{10}$ . Derivatives are full lines, whilst the displacements cooresponding to  $b = 64$ ,  $\tau = 10^{-3}$  and  $\tau_y = \{10^{-8}, 10^{-9}, 10^{-10}\}$  are the dashed lines. The trace expectation is shown as a full black line.

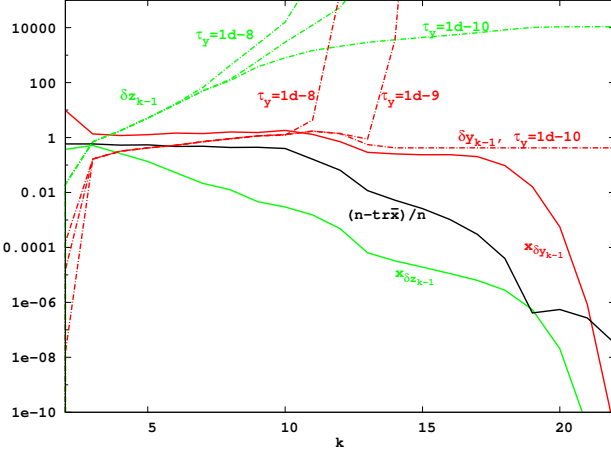


FIG. 3: Derivatives, displacements and the approximate trace of the scaled, singlelized NS iteration for a (3,3) nanotube with  $\kappa = 10^{10}$ . Derivatives are full lines, whilst the displacements cooresponding to  $b = 64$ ,  $\tau = 10^{-3}$  and  $\tau_y = \{10^{-3}, 10^{-4}, 10^{-6}\}$  are the dashed lines. The trace expectation is shown as a full black line.

In particular, the matrix  $S_1$ , being close to the identity, is better conditioned than  $S$  and computing  $S_1^{-1/2}$  requires much fewer Newton Schulz iterations. Moreover, since

$$\|(R_1 R_0) S (R_0 R_1) - I\|_F \lesssim \tau_1,$$

we see that  $R_1 R_0$  is a  $\tau_1$  approximation to  $S^{-1/2}$ . Notice that, from the stability bound for SpAMM, we can replace all of the exact matrix multiplications with SpAMM multiplications.

To formalize this, let  $S_0 = S$ , and suppose that  $R_j$  is the approximation to  $S_j^{-1/2}$  obtained via the Newton

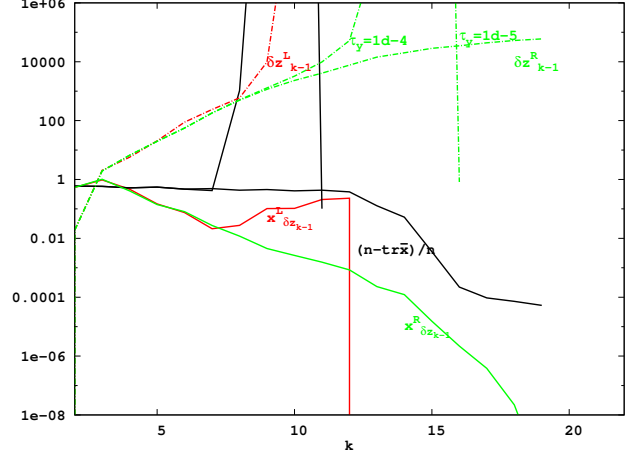


FIG. 4: Derivatives, displacements and the approximate trace of the unscaled, dual NS iteration for a (3,3) nanotube with  $\kappa = 10^{10}$ . Derivatives are full lines, whilst the displacements cooresponding to  $b = 64$ ,  $\tau = 10^{-3}$  and  $\tau_y = \{10^{-8}, 10^{-9}, 10^{-10}\}$  are the dashed lines. The trace expectation is shown as a full black line.

Schulz iteration with SpAMM tolerance  $\tau_j$ , so that

$$\|R_j \otimes_{\tau_j} S_j \otimes_{\tau_j} R_j - I\|_F \lesssim \tau_j.$$

Then define  $S_{j+1} = R_j \otimes_{\tau_K} S_j \otimes_{\tau_K} R_j$  and let  $R_{j+1}$  the approximation to  $S_{j+1}^{-1/2}$  obtained via the Newton Schulz iteration with SpAMM tolerance  $\tau_{j+1}$ , so that

$$\|R_{j+1} \otimes_{\tau_K} S_{j+1} \otimes_{\tau_K} R_{j+1} - I\|_F \lesssim \tau_{j+1}.$$

Then since  $S_{j+1} = R_j \otimes_{\tau_K} S_j \otimes_{\tau_K} R_j$ ,

$$\|R_{j+1} \otimes_{\tau_K} (R_j \otimes_{\tau_K} S_j \otimes_{\tau_K} R_j) \otimes_{\tau_K} R_{j+1} - I\|_F \lesssim \tau_{j+1}.$$

In general, defining

$$R_{\text{left}} \equiv R_{j+1} \otimes_{\tau_K} R_j \otimes_{\tau_K} R_{j-1} \cdots \otimes_{\tau_K} R_0,$$

and

$$R_{\text{right}} \equiv R_0 \otimes_{\tau_K} R_1 \cdots \otimes_{\tau_K} R_j \cdots \otimes_{\tau_K} R_{j+1},$$

it follows by induction that

$$\|R_{\text{left}} \otimes_{\tau_K} S \otimes_{\tau_K} R_{\text{right}} - I\|_F \lesssim \tau_K.$$

Now, by stability of SpAMM,

$$\|R_{\text{left}} S R_{\text{right}} - I\|_F \lesssim \tau_K.$$

Also,

$$R_{j+1} \otimes_{\tau_K} R_j \otimes_{\tau_K} R_{j-1} \cdots \otimes_{\tau_K} R_0$$

can be written as

$$(R_0 \otimes_{\tau_K} R_1 \cdots \otimes_{\tau_K} R_j \cdots \otimes_{\tau_K} R_{j+1})^T + \mathcal{O}(\tau_K).$$

Therefore,  $R_{\text{left}} = R_{\text{right}}^T + \mathcal{O}(\tau_K)$ , and so

$$\|R_{\text{left}} S R_{\text{left}}^T - I\|_F \lesssim \tau_K. \quad (32)$$

We can therefore write the following symbolic representation

$$S^{-1/2} = S_{\tau_{j+1}}^{-1/2} \otimes_{\tau_{j+1}} S_{\tau_j}^{-1/2} \otimes_{\tau_j} S_{\tau_{j-1}}^{-1/2} \cdots \otimes_{\tau_1} S_{\tau_0}^{-1/2} + \mathcal{O}(\tau_{j+1}),$$

where  $S_{\tau_k}^{-1/2}$  is a  $\tau_k$  approximation to the inverse square root of  $S_k = S_{\tau_{k-1}}^{-1/2} \otimes_{\tau_{k-1}} S_{k-1} \otimes_{\tau_j} S_{\tau_{k-1}}^{-1/2}$ .

## VI. ITERATED REGULARIZATION

Shown in the preceding section, singleliliy limits application of the NS square root iteration under agresive SpAMM approximation. These limits can be circumvented through Tikhonov regularization [], involving a small level shift of eigenvalues,  $s_\mu \leftarrow s + \mu I$ , leading to a more well conditioned matrix with  $\kappa(s_\mu) = \frac{\sqrt{s_{N-1}^2 + \mu^2}}{\sqrt{s_0^2 + \mu^2}}$  []. However, achieving substantial acceleration with severe ill-conditioning may require a large level shift, producing inverse factors of little practical use. One approach to recover a more accurate inverse factor is Riley's method []:

$$s^{-1/2} = s_\mu^{-1/2} \cdot \left( I + \frac{\mu}{2} s_\mu^{-1} + \frac{3\mu^2}{8} s_\mu^{-2} + \dots \right), \quad (33)$$

but this is ineffective when  $\mu$  is large, and invovles powers of the full inverse.

Here, we outline an alternative, nested product representation of the inverse factor and show preliminary results for a first, most approximate solution. This most approximate (but effective) solution is (ideally) representative of one order in the precision,  $\tau_0 \sim .1$ , and corrective by one order in the condition,  $\mu_0 \sim .1$ , yeilding a thin, 0<sup>th</sup> preconditioner,  $s_{\tau_0 \mu_0}^{-1/2}$ . This "thin" iteration may bring spectral resolution into alignment with norm magnitudes towards the resolvent  $I_{\tau_0 \mu_0} \equiv \tilde{I}(s_{\tau_0 \mu_0})$ , strengthening Eq. (5).

Culled SpAMM volumes for this most approximate solution are shown with increasing system size in Fig. VI for the single instance, and in Fig. VI for the dual instance, cooresponding to "thin NS" iteration for the (3,3)  $\kappa(s) = 10^{10}$  nanotube series. The behavior of these instances is very different; in the "single" instance, a single iteration could not be found at precision  $\tau_0 = .1$ , even with  $\mu_0 = .1$  regularization. Also, this single iteration sees a weakly convergent trace with inflating cull-volumes. On the other hand, volume of the dual iteration is strongly contracted with resolution of the identity.

These results reflect very different cull-spaces. In the single instance, the spectral resolution of powers is not compresive, and  $\tilde{y}_k^{\text{single}} \rightarrow s_{\tau_0 \mu_0}^{-1/2} \otimes_{\tau_0} s_{\mu_0}$  is poorly bound by Eq. (5). In the dual case however,  $\tilde{y}_k^{\text{dual}} \rightarrow$

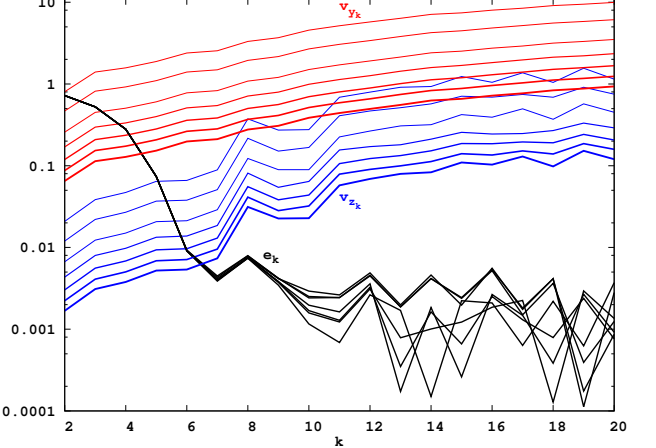


FIG. 5: Culled volumes in the thin slice, single instance approximation of  $s_{\tau_0 \mu_0}^{-1/2}$  for the (3,3) nanotube,  $\kappa(s) = 10^{10}$  matrix series described in Section B. In the "single" instance, it was not possible to achieve stability with  $\tau_0 = .1$ . In this "single" case, a thin slice cooresponds to  $\mu_0 = .1$ ,  $\tau_0 = 10^{-2}$  &  $\tau_s = 10^{-4}$ , and volumes are  $v_{\tilde{z}_k} = (\text{vol}_{\tilde{z}_{k-1} \otimes_{\tau} h[\tilde{x}_{k-1}]} \times 100\% / N^3)$  and  $v_{\tilde{y}_k} = (\text{vol}_{s \otimes_{\tau_s} \tilde{z}_k} \times 100\% / N^3)$ . Line width increases with increasing system size. Also shown is the trace error,  $e_k = (N - \text{tr } \mathbf{x}_k) / N$ .

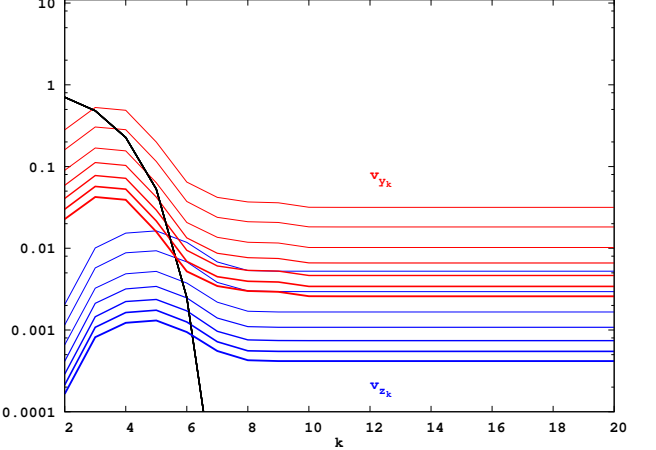


FIG. 6: Culled volumes in the thin slice, dual instance approximation of  $s_{\tau_0 \mu_0}^{-1/2}$  for the (3,3) nanotube,  $\kappa(s) = 10^{10}$  matrix series described in Section B. The thin slice cooresponds to  $\mu_0 = .1$ ,  $\tau_0 = .1$  &  $\tau_s = .001$  with volumes  $v_{\tilde{y}_k} = (\text{vol}_{h[\tilde{x}_{k-1}] \otimes_{\tau_s} \tilde{y}_k} \times 100\% / N^3)$  and  $v_{\tilde{z}_k} = (\text{vol}_{\tilde{z}_{k-1} \otimes_{\tau} h[\tilde{x}_{k-1}]} \times 100\% / N^3)$ . Line width increases with increasing system size. Also shown is the trace error,  $e_k = (N - \text{tr } \mathbf{x}_k) / N$ , which rapidly approaches  $10^{-11}$  (not shown).

$I_{\tau_0 \mu_0} \otimes_{\tau_0} s_{\tau_0 \mu_0}^{1/2}$  and  $\tilde{z}_k^{\text{dual}} \rightarrow s_{\tau_0 \mu_0}^{-1/2} \otimes_{\tau_0} I_{\tau_0 \mu_0}$ , with Eq. (5) tightening to

$$\Delta^{I_{\tau_0 \mu_0} \cdot s_{\tau_0 \mu_0}^{1/2}} < \tau n \|s_{\tau_0 \mu_0}^{1/2}\| \quad (34)$$

and

$$\Delta s_{\tau_0 \mu_0}^{-1/2} \cdot I_{\tau_0 \mu_0} < \tau n \|s_{\tau_0 \mu_0}^{-1/2}\|, \quad (35)$$

as relative and absolute errors converge. This tightening is compressive, leading to complexities that are quadtree copy in place.

In the dual instance, the SpAMM approximation can be brought all the way to  $\tau_0 = .1$  in the case of  $\mu_0 = .1$ . From this first slice  $s_{\tau_0, \mu_0}^{-1/2}$  then, a next level shifted preconditioner can be found,  $s_{\tau_0 \mu_1}^{-1/2}$ , based on the residual  $(s_{\tau_0 \mu_0}^{-1/2})^\dagger \otimes_{\tau_0} (s + \mu_1 I) \otimes_{\tau_0} s_{\tau_0 \mu_0}^{-1/2}$ , with e.g.  $\mu_1 = .01$ . It may then be possible to find the full (SpAMM most approximate) factor as the nested product of preconditioned thin slices;

$$s_{\tau_0}^{-1/2} = s_{\tau_0 \mu_n}^{-1/2} \otimes_{\tau_0} s_{\tau_0 \mu_{n-1}}^{-1/2} \otimes_{\tau_0} \dots \otimes_{\tau_0} s_{\tau_0 \mu_0}^{-1/2} \quad (36)$$

In this way, iterative regularization can be used to find a product representation of the inverse square root at a SpAMM resolution potentially far more permissive than otherwise possible. Likewise, it may be possible to obtain the full factor with increasing SpAMM resolution in the product representation:

$$s^{-1/2} = s_{\tau_m}^{-1/2} \otimes_{\tau_m} s_{\tau_{m-1}}^{-1/2} \otimes_{\tau_{m-1}} \dots \otimes_{\tau_0} s_{\tau_0}^{-1/2} \quad (37)$$

taken over the sequence  $1 > \tau_0 > \tau_1 > \dots > \tau_n$ . More generally,

$$s^{-1/2} \equiv \bigotimes_{\substack{\tau=\tau_0 \\ \mu=\mu_0}} |\tau \mu; s^{-1/2}\rangle, \quad (38)$$

acknowledging the potential for a flexible path between precision and regularization. The bracket notation marks the potential for assymmetries in the intermediate representation.

This thin product representation may have advantages: (1) Each thin solve involves a few generic and well behaved steps that may be narrowly optimized; (2) Each thin solve can be brought rapidly into compressive identity iteration; (3) The SpAMM bound is vastly strengthened, via Eqs. (34-35); (4) A new algebraic  $n$ -body form of locality is exploited; (5) The inverse factor can be applied incrementally; (6) Slice update and application is ammenable to continous temporal partitioning based on e.g. persistence data.

## VII. LOCALITY

Astrophysical  $n$ -body algorithms employ range queries over spatial databases to hierarchically discover and compute approximations that commit only small errors. Often, these spatial databases are ordered with a space filling curve (SFC) [], which maps points that are close in

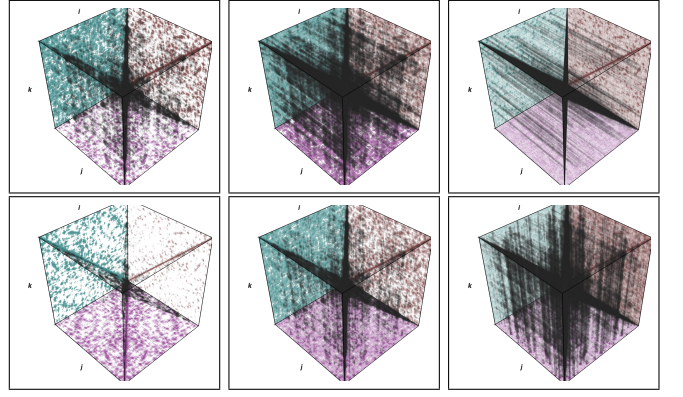


FIG. 7: The  $ijk$  task and data space for construction of the unregularized preconditioner  $|\tau_0 = .001, \mu_0 = .0; s^{-1/2}\rangle$ , with dual instance square root iteration, and for the 6-311G\*\* metric of 100 periodic water molecules at STP. At top its  $y_k = h_\alpha[x_{k-1}] \otimes_{\tau_0} y_{k-1}$  for  $k = 0, 4, \& 15$ , while on the bottom we have  $x_k = y_k \otimes_{\tau} z_k$  for  $k = 0, 4, \& 15$ . Maroon is  $a$ , purple is  $b$ , green is  $c$ , and black is the volume  $\text{vol}_{a \otimes_{\tau} b}$  in the product  $c = a \otimes_{\tau} b$ .

space to an index where they are also close. The block-by-magnitude structures empowering the SpAMM approximation are *metric localities*; in quantum chemical examples they coorespond to an underlying SFC ordering of Cartesian coordinates.

Warren and Salmon showed how to parlay spatial locality into temporal locality, remapping and repartitioning the space filling curve to rebalance distributed  $n$ -body tasks, based on accumulated histories (persistence data). In a similar way, we showed how persistence can be used to achieve strong parallel scaling for SpAMM with commonly available runtimes []. Persistence data, providing temporal locality, may also be useful in mathematical approximation.

In Figure 7, we show  $\otimes_{\tau}$  volumes for square root iteration, cooresponding to the metric of a small, periodic water box with the large, 6-311G\*\* basis. For the 3-d periodic case, diminishing Cartesian seperations lead to long-skinny delocalizations (pillae) and much denser matrices, relative to e.g. a one-dimensional nano-tube. These delocalizations coorespond to weakness in Eq. (5), and to the tighter thresholds required to maintain a single iteration in the MAYSS approximation. This effect is even more pronounced in the single instance (not shown), where delocalizations are exaggerated due to spectral resolutions that are broader. Eventually, Cartesian seperation will thin and trim the density of these delocalizations, leading to complexity reduction based on the effects of metric locality alone, as demonstrated in ??.

In Figures 8 and 9, we show a new kind of locality that is uniquely exploited by  $n$ -body approximation of the square root iteration. This algebraic locality develops compressively towards convergence as the contractive identity iteration develops. We call this compression *lensing*, involving collapse of the culled volume about

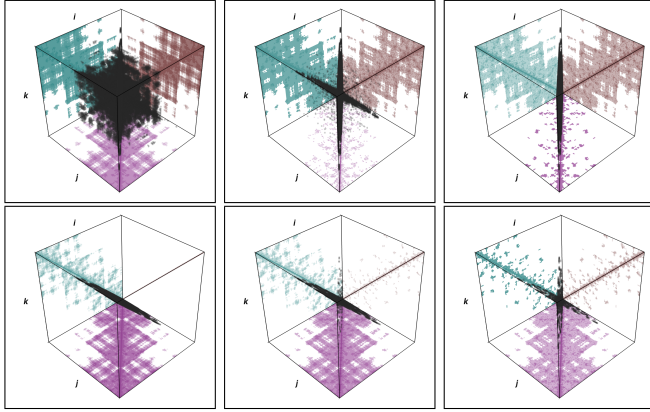


FIG. 8: The  $ijk$  task and data space for construction of the MAYEBOO preconditioner  $|\tau_0 = .1, \mu_0 = .1; s^{-1/2}\rangle$ , with dual instance square root iteration, and for an  $8 \times U.C.$  (3,3)  $\kappa(s) = 10^{11}$  nanotube.  $\mathbf{y}_k$  appears wider than  $\mathbf{z}_k$  because it is computed at a higher precision,  $\tau_s = .001$ , and because the first multiply involves  $s^2$ . At top its  $\mathbf{y}_k = h_\alpha[\mathbf{x}_{k-1}]_{\otimes \tau_s} \mathbf{y}_{k-1}$  for  $k = 0, 4, \& 16$ , while on the bottom we have  $\mathbf{x}_k = \mathbf{y}_k \otimes \tau \mathbf{z}_k$  for  $k = 0, 2, \& 16$ . Maroon is  $\mathbf{a}$ , purple is  $\mathbf{b}$ , green is  $\mathbf{c}$ , and black is the volume  $\text{vol}_{a \otimes \tau b}$  in the product  $\mathbf{c} = \mathbf{a} \otimes \tau \mathbf{b}$ .

plane diagonals of the resolvent. Lensing corresponds to strengthening of Eq.(??) to yeild Eqs. (34) and (35), and strong convergence of the directional derivatives Eq.(??-??) to **0**. This is an important, mitigating computational effect for the  $\mathbf{y}_k$  channel that involves the tighter threshold,  $\tau_s \sim 0.01 \times \tau$ .

In addition, non-Euclidian measures are relevant for achieving metric locality in the SpAMM algebra, including information measures, space filling curve generalizations, as well as graph reorderings that envelope matrix elements about the diagonal  $\mathbb{I}$ , a common approach in structural mechanics. In Figure 12 we show development of a first, unregularized preconditioner for such an example; the structural matrix  $\mathbf{s} = \text{bcsstk14}$  is a  $\kappa(\mathbf{s}) = 10^{10}$  matrix cooresponding to the roof of the Omni Coliseum in Atlanta  $\mathbb{I}$ . These results show remarkable gossamer sheeting and flattening along plane diagonals, at top for developmentent of  $\mathbf{y}_k$ , and hollow accumulation of  $\text{vol}_{\mathbf{y}_k \otimes \tau \mathbf{z}_k}$  looking down at  $\mathbf{y}_k$  (along bottom).

## VIII. SUMMARY

In this contribution, we developed the  $n$ -body solver SpAMM for square root iteration. The  $n$ -body solver carries out metric queries with occlusion-culling based on a modified Cauchy-Schwarz criterion, Eq. ??, with a bounded relative error in the product, given by Eq. ???. SpAMM exploits metric locality, cooresponding to decay with Cartesian or non-Euclidian seperation, and also algebraic locality, developing with identity iteration.

The SpAMM query hierarchically resolves complex algebraic structures in the product space of square root iteration, culling out the  $i = k$  and  $i = k$  planes and along

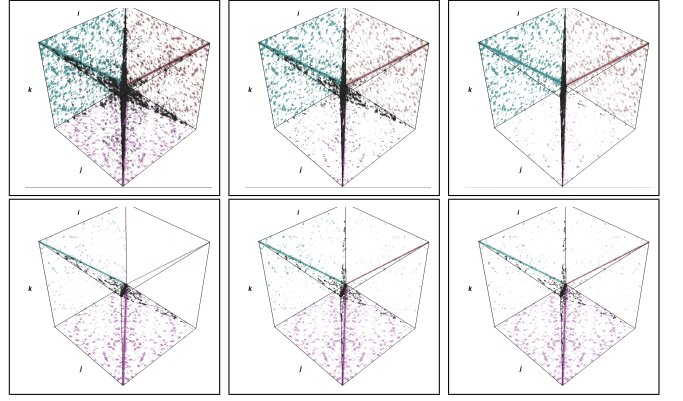


FIG. 9: The  $ijk$  task and data space for construction of the MAYEBOO preconditioner  $|\tau_0 = .1, \mu_0 = .1; s^{-1/2}\rangle$ , with dual instance square root iteration and for 6-311G\*\* metric of 100 periodic water molecules at STP. At top its  $\mathbf{y}_k = h_\alpha[\mathbf{x}_{k-1}]_{\otimes \tau_s} \mathbf{y}_{k-1}$  for  $k = 0, 4, \& 16$ , while on the bottom we have  $\mathbf{x}_k = \mathbf{y}_k \otimes \tau \mathbf{z}_k$  for  $k = 0, 4, \& 16$ . Maroon is  $\mathbf{a}$ , purple is  $\mathbf{b}$ , green is  $\mathbf{c}$ , and black is the volume  $\text{vol}_{a \otimes \tau b}$  in the product  $\mathbf{c} = \mathbf{a} \otimes \tau \mathbf{b}$ .

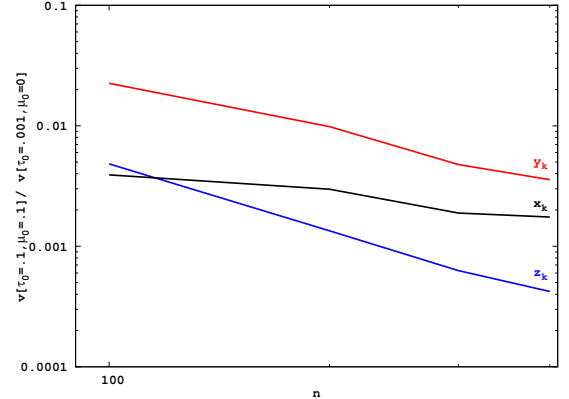


FIG. 10: Complexity reduction in metric square root iteration for periodic 6-311G\*\* water. Shown is the ratio of lensed product volumes for the regularized most-approximate-yet-effective-by-one-order (MAYEBOO) approximation and the unregularized most-approximate-yet-still-stable (MAYSS) approximation.

the  $ijk$  cube-diagonal. In the case of the dual  $\mathbf{y}_k$  and  $\mathbf{z}_k$  channels, these structures contract further as multiplication by near-identity is reached, with *lensing* about the plane diagonal and computational complexities tending towards quadtree-copy-in-place.

In Section ??, we looked at stability leading to the basin of convergence and sensitivity of the three product channels  $\mathbf{y}_k$ ,  $\mathbf{z}_k$  and  $\mathbf{x}_k$ , for the SpAMM approximation in the canonical “dual” instance, Eq. (??), and for the “single” instance, Eq. (??). Consistent with HMMT  $\mathbb{I}$ , the  $\mathbf{z}_k$  channel is sensitized by the full inverse,  $\mathbf{s}^{-1}$ , requiring a tighter threshold for that case,  $\tau_s \ll \tau$ . Later, we find that extra cost is strongly mitigated by lensing. Also in Section ??, we looked at bifurcations of scaled

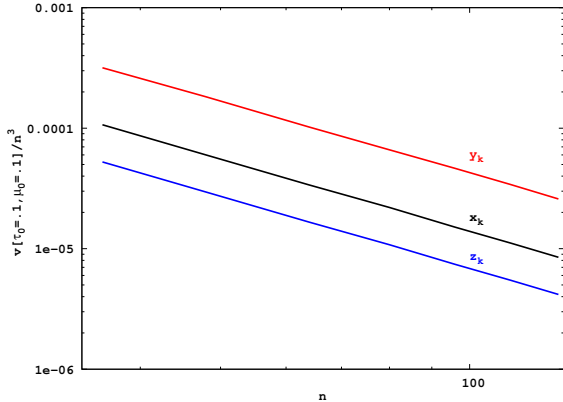


FIG. 11: Complexity reduction in metric square root iteration for periodic 6-311G\*\* water. Shown is the ratio of lensed product volumes for the regularized most-approximate-yet-effective-by-one-order (MAYEBOO) approximation and the unregularized most-approximate-yet-still-stable (MAYSS) approximation.

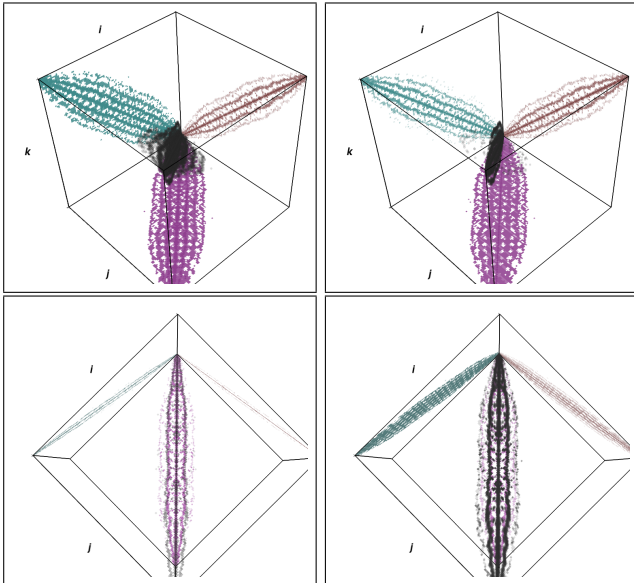


FIG. 12: The  $ijk$  task and data space for construction of the unregularized preconditioner  $|\tau_0 = .001, \mu_0 = .0; s^{-1/2}\rangle$ , with the dual instance of square root iteration and for 6-311G\*\* metric of 100 periodic water molecules at STP. At top its  $\mathbf{y}_k = h_\alpha[\mathbf{x}_{k-1}] \otimes_{\tau_s} \mathbf{y}_{k-1}$  for  $k = 0, 4, & 15$ , while on the bottom we have  $\mathbf{x}_k = \mathbf{y}_k \otimes_{\tau_s} \mathbf{z}_k$  for  $k = 0, 4, & 15$ . Maroon is  $\mathbf{a}$ , purple is  $\mathbf{b}$ , green is  $\mathbf{c}$ , and black is the volume  $\text{vol}_{\mathbf{a} \otimes_{\tau_s} \mathbf{b}}$  in the product  $\mathbf{c} = \mathbf{a} \otimes_{\tau_s} \mathbf{b}$ .

and unscaled iterations for ill-conditioned systems, towards a most-approximate-yet-still-stable (MAYSS) preconditioner, and dissected competing effects at the edge of stability, between compounding displacement magnitudes and strongly convergent directional derivatives.

In Section ??, we proved that at convergence Eq. (5) tightens significantly, corresponding to a lensing orbit. Then, we introduced iterated regularization for

ill-conditioning, and showed how the full inverse factor can be achieved by products of generic, regularized, well conditioned and increasingly more accurate solutions;  $s^{1/2} = \bigotimes_{\mu} |\mu, \tau; s^{-1/2}\rangle$  cooresponding to a first most-approximate-yet-effective-by-one-order (MAYEBOO) preconditioner  $|\mu = .1, \tau = .1; s^{-1/2}\rangle$ . We looked at the MAYEBOO approximation for both the single and dual instances, and found that even with the most permissive regularization, spectral resolution in the single instance is too broad to achieve strong lensing.

Finally, we looked at the MAYSS and MAYBOO approximations for periodic water systems, for ill-conditioned nanotubes, and for the ill-conditioned structural matrix `bcsstk14` for the Omni Coliseum in Atlanta []. For the problem of large basis periodic water systems, we find a MAYBOO/MAYSS volume compression of two to three orders. For the problem of an ill-conditioned nano-tube, we find a MAYBOO/MAYSS volume compression of ... Remarkably, the ill-conditioned `bcsstk14` was able to achieve a strongly lensed state in the MAYSS approximation, with remarkable gossamer sheeting and flattening along plane diagonals, and hollow, reticulate volumes of the resolvent.

## IX. CONCLUSIONS

This work is gauged against other methods for fast matrix multiplication discussed in Section ???. Against SpMM, the  $n$ -body approach offers a bounded control over relative errors in the product and the ability to resolve complex algebraic structures, about plane-diagonals of the  $ijk$ -cube, along tall-skinny pillae and for volumetric contractions to lower dimensional objects via lensing. The  $n$ -body method uniquely and synergistically exploits two distinct forms of locality, metric locality cooresponding to a Cartesian or non-Euclidean decay principle, and algebraic locality cooresponding to contractive identity iteration. Also, strong parallel scaling for the  $\mathcal{O}(n)$  electronic structure problem has been demonstrated with the SpAMM kernel, a feature that remains elusive for methods based on SpMM [? ].

Against methods for matrix compression [], as well as against Fast Matrix Multiplication of the Strassen type [], the quadtree data structure and the octree task space employed by SpAMM are entirely complimentary. In the case of sketch products [], persistence data can be used to identify and characterize pillae resulting from broad spectral resolutions; then, it may be possible to deploy streaming approaches for these tall-skinny delocalizations []. Thus, the concurrent application of fast methods for matrix multiplication may be enabled by the database framework supporting  $n$ -body approximations.

Beyond the fast matrix multiply,  $n$ -body frameworks may enable additional, layered functionalities and economizations in complex solver ecosystems, with facile interoperability and mathematical agility, through generic recursion and skelitization, and with common runtimes

able to exploit temporal and data localities. For example, we recently generalized SpAMM recursion to the problem of Fock-exchange, with a recursive triple (hextree) metric query on the Almlöf-Alhrichs direct SCF criteria []. Also, mathematical equivalence with the matrix sign function, Eq. (??), and close structural relationships with the polar decomposition may enable to extend functionality of the  $n$ -body iterations developed here.

Despite these compelling features and related xxx,  $n$ -body square-root iteration must be gauged by its ability to compute a high quality inverse factor. Here, we have only looked at complexity and stability of the most approximate preconditioners; the most-approximate-yet-still-stable (MAYSS) approximation and the regularized most-approximate-yet-effective-by-one-order (MAYEBOO) approximations. However, these results are encouraging, showing the potential for several to many orders of magnitude reduction in complexity for the regularized approximation relative to the unregularized approximation, made possible by construction of a much lower precision preconditioner than would otherwise be possible, via Eq. (??), and also by operations in the strongly contractive regime, under Eqs. (34–35). These and related preliminary results [] suggest that a SpAMM sandwich of thin, generic iterations may enable a competitive computational approach that avoids explicit computation of the ill-conditioned factor.

## Appendix A: Implementation

FP, F08, OpenMP 4.0 In the current implementation, all persistence data (norms, flops, branches & etc.) are

accumulated compactly in the backward recurrence. This persistence data that may be achieved by minimal locally essential trees [].

For these reasons, maintaining connection to the eigenvectors of  $s$  through a tighter first product is necessary. In the single instance, and with a tighter “ $s$ ” product,  $\tau_s \ll \tau$ , we find very interesting left/right differences; namely, the right first product

$$\tilde{\mathbf{x}}_k^R \leftarrow \tilde{\mathbf{z}}_k^\dagger \otimes_\tau (s \otimes_{\tau_s} \tilde{\mathbf{z}}_{k-1}) , \quad (\text{A1})$$

is different from the left first product

$$\tilde{\mathbf{x}}_k^L \leftarrow \left( \tilde{\mathbf{z}}_k^\dagger \otimes_{\tau_s} s \right) \otimes_\tau \tilde{\mathbf{z}}_{k-1} . \quad (\text{A2})$$

damping the inversion and the small value to be added c is called Marquardt-Levenberg coefficient

Map switching and etc based on TrX

## Appendix B: Data

3.3 carbon nanotube with diffuse  $sp$ -function double exponential (Fig.)

- 
- [1] O. Penrose and J. Lebowitz, Commun. Math. Phys. **184** (1974).
  - [2] J. Voit, *The Statistical Mechanics of Financial Markets*, Theoretical and Mathematical Physics (Springer Berlin Heidelberg, 2006), ISBN 9783540262893, URL <https://books.google.com/books?id=6zUlh\TkWSwC>.
  - [3] L. Anselin, Int. Reg. Sci. Rev. **26**, 153 (2003), ISSN 01600176, URL <http://irx.sagepub.com/cgi/doi/10.1177/0160017602250972>.
  - [4] J. Hardin, S. R. Garcia, and D. Golan, Ann. Appl. Stat. **7**, 1733 (2013), ISSN 1932-6157, arXiv:1106.5834v4.
  - [5] I. Krishtal, T. Strohmer, and T. Wertz, Found. Comput. ... (2013), ISSN 1615-3375.
  - [6] P. O. Lowdin, Advances in Physics **5**, 1 (1956).
  - [7] A. R. Naidu, p. 1 (2011), 1105.3571.
  - [8] N. J. Higham, *Functions of Matrices* (Society for Industrial & Applied Mathematics,, 2008).
  - [9] F. G. Gustavson, ACM Transactions on Mathematical Software (TOMS) **4**, 250 (1978).
  - [10] S. Toledo, IBM J. Res. Dev. **41**, 711 (1997).
  - [11] M. Challacombe, Comput. Phys. Commun. **128**, 93 (2000).
  - [12] D. R. Bowler and T. M. and M. J. Gillan, Comp. Phys. Comm. **137**, 255 (2000).
  - [13] M. Benzi and M. Tuma, Appl. Numer. Math. **30**, 305 (1999).
  - [14] M. Benzi, J. Comput. Phys. **182**, 418 (2002).
  - [15] D. R. Bowler and T. Miyazaki, Reports Prog. Phys. **75**, 36503 (2012).
  - [16] M. Benzi, P. Boito, and N. Razouk, SIAM Rev. **55**, 3 (2013).
  - [17] V. Strassen, Numer. Math. **13**, 354 (1969).
  - [18] G. Ballard, J. Demmel, O. Holtz, and O. Schwartz, Communications of the ACM **57**, 107 (2014).
  - [19] A. G. Gray and A. W. Moore, in *Advances in Neural Information Processing Systems* (MIT Press, 2001), vol. 4, pp. 521–527, URL <http://citeseerx.ist.psu.edu/viewdoc/summary?doi=10.1.1.28.7138>.
  - [20] A. Gray (2003), URL <http://reports-archive.adm.cs.cmu.edu/anon/anon/2003/abstracts/03-222.html>.
  - [21] T. Sarlos, In Proceedings of the 47th Annual IEEE Symposium on Foundations of Computer Science (FOCS) (2006).
  - [22] P. Drineas, R. Kannan, and M. W. Mahoney, SIAM Journal on Computing **36**, 132 (2006).
  - [23] M. W. Mahoney, pp. 1–53 (2012), arXiv:1502.03032v1.

- [24] R. Pagh, ACM Trans. Comput. Theory **5**, 1 (2013).
- [25] J. V. T. Sivertsen (2014).
- [26] D. P. Woodruff, **10**, 1 (2015), arXiv:1411.4357v3.
- [27] P. Mishra and M. H. Eich, ACM Comput. Surv. **24**, 63 (1992).
- [28] E. G. Hoel and H. Samet, in *Parallel Processing, 1994. ICPP 1994. International Conference on* (1994), vol. 3, pp. 227–234.
- [29] E. H. Jacox and H. Samet, ACM Trans. Database Syst. **28**, 230 (2003).
- [30] S. Chen, A. Ailamaki, P. B. Gibbons, and T. C. Mowry, ACM Trans. Database Syst. **32** (2007).
- [31] R. R. Amosson and R. Pagh, in *Proceedings of the 12th International Conference on Database Theory* (ACM, 2009), pp. 121–126.
- [32] M. D. Lieberman, J. Sankaranarayanan, and H. Samet, in *Proceedings of the 2008 IEEE 24th International Conference on Data Engineering* (IEEE Computer Society, Washington, DC, USA, 2008), pp. 1111–1120, ISBN 978-1-4244-1836-7.
- [33] C. Kim, T. Kaldewey, V. W. Lee, E. Sedlar, A. D. Nguyen, N. Satish, J. Chhugani, A. Di Blas, and P. Dubey, Proc. VLDB Endow. **2**, 1378 (2009).
- [34] Z. Bai and J. Demmel, SIAM J. Matrix Anal. Appl. **19**, 205 (1998).
- [35] N. J. . Higham, N. M. D . Steven Mackey, and F. . coise Tisseur, SIAM J. Matrix Anal. Appl. **26**, 849 (2005).
- [36] J. Chen and E. Chow, Preprint ANL/MCS-P5059-0114, Mathematics and Computer Science Division, Argonne National Laboratory, Argonne, IL 60439 (2014).
- [37] V. Pan and R. Schreiber, SIAM J. Sci. Stat. Comput. (1991).